

Trichomonas Vaginalis Induces Apoptosis via ROS and ER Stress Through ER-mitochondria Crosstalk in Human Cervical Epithelial Cells

Fei Fei Gao

Chungnam National University

Juan-Hua Quan

Affiliated Hospital of Guangdong Medical University

Min A Lee

Chungnam National University

Wei Ye

Affiliated Hospital of Guangdong Medical University

Jae-Min Yuk

Chungnam National University

Guang-Ho Cha

Chungnam National University

In-Wook Choi

Chungnam National University

Young-Ha Lee (✉ yhalee@cnu.ac.kr)

Chungnam National University School of Medicine

Research Article

Keywords: Trichomonas vaginalis, Human cervical epithelial SiHa cells, Endoplasmic reticulum stress, Mitochondrial apoptosis, Reactive oxygen species

Posted Date: March 22nd, 2021

DOI: <https://doi.org/10.21203/rs.3.rs-330817/v1>

License:  This work is licensed under a Creative Commons Attribution 4.0 International License.

[Read Full License](#)

Abstract

Background: Human trichomoniasis is one of the most common sexually transmitted infections; however, its pathogenesis remains unclear. Here, we investigated the role of the endoplasmic reticulum (ER) in apoptosis induction by *T. vaginalis* in human cervical epithelial SiHa cells

Methods: We evaluated the cytotoxicity, apoptosis, reactive oxygen species (ROS) production, mitochondrial membrane potential (MMP), ER stress response, and Bcl-2 family protein expressions using LDH assay, immunocytochemistry, flow cytometry, JC-1 dye staining, and western blotting.

Results: *T. vaginalis* induced LDH-dependent cytotoxicity, mitochondrial ROS production, and apoptosis in SiHa cells, parasite burden- and infection time-dependently. *T. vaginalis* also induced ER stress response and mitochondrial dysfunction, such as MMP depolarization and imbalance in levels of Bcl-2 family proteins, in SiHa cells in a parasite burden- and infection time-dependent manner. Pretreatment with *N*-Acetyl cysteine (ROS scavenger) or 4-phenylbutyric acid (4-PBA, ER stress inhibitor) significantly alleviated apoptosis, ROS production, mitochondrial dysfunction, and ER stress response in a dose-dependent manner. These data suggested that SiHa cell apoptosis is affected by ROS and ER stress after *T. gondii* infection. In addition, *T. vaginalis* induced ASK1 and JNK phosphorylation in SiHa cells, however 4-PBA or SP600125 (JNK inhibitor) pretreatment significantly attenuated ASK1/JNK phosphorylation, mitochondrial dysfunction, apoptosis, and ER stress response in SiHa cells, dose-dependently.

Conclusions: *T. vaginalis* induces mitochondrial apoptosis via ROS and parasite-mediated ER stress via the IRE1/ASK1/JNK/Mcl-1 pathways, and also induces ER stress response directly and mitochondrial ROS-dependently in human cervical epithelial SiHa cells, thus, *T. vaginalis* induces apoptosis via ROS and ER stress through ER-mitochondria crosstalk in human cervical epithelial cells. These results expand our understanding of the molecular mechanisms underlying the pathogenesis of human trichomoniasis.

Background

Trichomonas vaginalis is a flagellated protozoan parasite that infects the female reproductive tract and the male urethra [1]. It causes the most common, curable, and non-viral sexually transmitted infection (STI) worldwide. The World Health Organization (WHO) estimated 156 million cases of *T. vaginalis* infection worldwide in 2016, accounting for almost half of the global STI incidence [2]. The parasite causes vaginitis and cervicitis in women and asymptomatic urethritis and prostatitis in men. In addition, the host inflammatory response against this parasite is predicted to fuel multiple adverse health effects, such as high incidence of premature births [3], increased risk of cervical cancer [4], and increased susceptibility to human immunodeficiency virus infection [5]. However, the pathogenesis for *T. vaginalis* infection is poorly understood.

Apoptosis, a cellular event induced by the activation of a series of enzymes known as caspases, occurs when a cell is damaged beyond repair, infected with a pathogen, or stressed due to DNA damage or toxic chemicals [6]. Mitochondria are important in the regulation and transmission of apoptotic signals, which

are regulated by maintaining a balance between the levels of the Bcl-2-family proteins [7]. Several studies have presented various mechanisms behind the induction of apoptosis by *T. vaginalis* infection using in vitro models. *T. vaginalis*-induced apoptosis of cells has been described via the production of reactive oxygen species (ROS) [8, 9], secretion of cysteine proteases from *T. vaginalis* [10–12], upregulation of proapoptotic molecules including Fas, TRAIL and TRAILR1 [13], mitochondrial dysfunction, including alternation of mitochondrial membrane potential (MMP) and expression of Bcl-2 family proteins [14, 15], or activation of the p38 MAPK pathway [16]. However, the role of endoplasmic reticulum (ER) in *T. vaginalis*-induced apoptosis has not been elucidated.

ROS function as intermediates in cellular processes, such as inflammatory responses, cell cycle progression, apoptosis, aging, and cancer; they are produced in various organelles and via different enzyme systems, including mitochondria, ER, peroxisomes, and NADPH oxidase (NOX). Mitochondrion is the major source of ROS [17]. ER-mitochondria crosstalk is critical in regulating cell metabolism and cell death [18, 19]. Previous reports have shown that ROS are produced in *T. vaginalis*-infected human neutrophils and cervical epithelial cells and induce apoptosis [8, 9]; it has also been shown that they activate NLRP3 inflammasome formation in human prostate epithelial REPE-1 cells [20]. However, the role of ER in ROS-induced apoptosis by *T. vaginalis* infection has not been studied.

The ER plays a role in protein folding and assembly, lipid biosynthesis, vesicular traffic, and cellular calcium storage. Its function can be disturbed by various factors, such as the inhibition of protein glycosylation, calcium depletion, changes in redox status, and expression of misfolded proteins or unfolded proteins [21]. Uncontrolled severe oxidative stress triggers a series of pro-apoptotic signaling pathways, including ER stress and mitochondrial dysfunction, which ultimately results in cell apoptosis [21–23]. Many researchers have characterized the role of ER stress in cells infected by viruses and bacteria [24–26]. In addition, ER stress has been investigated in cells infected by protozoan parasites, including *Plasmodium*, *Toxoplasma*, *Cryptosporidium*, and *Leishmania* [27]; however, there has been no such study on cells infected with *T. vaginalis*.

Therefore, in this study, we aimed to investigate the role of ER stress response in combination with mitochondria in *T. vaginalis*-infected human cervical epithelial SiHa cells. We evaluated the cytotoxicity, apoptosis, ROS production, MMP, ER stress response, and Bcl-2 family protein levels in *T. vaginalis*-infected SiHa cells with or without specific inhibitors using lactate dehydrogenase (LDH) assay, immunocytochemistry, flow cytometry, JC-1 dye staining, and western blotting.

Methods

Reagents and antibodies.

CytoTox 96[®] Non-Radioactive Cytotoxicity Assay was obtained from Promega (Madison, WI, USA). CellROX[®] Oxidative Stress Reagents was purchased from Life Technologies (Alfagene, Carcavelos, Portugal). MitoSOXTM red mitochondrial superoxide indicator was purchased from ThermoFisher

Scientific (Waltham, MA, USA). JC-1 MitoMP detection kit was obtained from Dojindo (Kumamoto, Kumamoto, Japan). The ER stress inhibitor, 4-PBA, the ROS scavenger NAC and the JNK inhibitor SP600125 were purchased from Sigma Chemical Co. (St. Louis, MO, USA).

ER Stress Antibody Sampler Kit, anti-activating transcription factor 6 (ATF6), anti-phospho protein kinase RNA-like endoplasmic reticulum kinase (p-PERK), anti-phospho eukaryotic translation initiation factor 2a (p-eIF2 α), anti-poly (ADP-ribose) polymerase (PARP), anti-cleaved caspase-3, pro-Apoptosis Bcl2 Family Member Antibody Sampler Kit, pro-Survival Bcl2 Family Member Antibody Sampler Kit, anti-phospho-apoptosis signal-regulating kinase 1 (p-ASK1, Ser967), anti-phospho-ASK1 (Thr845), anti-ASK1, anti-phospho c-Jun N-terminal kinase (p-JNK, Thr183/Tyr185), anti-JNK (56G8), anti- β -actin antibodies were purchased from Cell Signaling Technology Inc. (Danvers, MA, USA). Anti-CCAAT/enhancer-binding protein-homologous protein (CHOP), and anti-phospho inositol-requiring protein 1a (p-IRE1 α) antibodies were obtained from Abcam (Cambridge, MA, USA). The following secondary antibodies, anti-rabbit-horseradish peroxidase (HRP) and anti-mouse-HRP, were from Jackson Immuno Research Laboratories (West Grove, PA, USA). Goat anti-Mouse IgG (H + L) Highly Cross-Adsorbed Secondary Antibody–Alexa Fluor 568 was from ThermoFisher Scientific (Waltham, MA, USA).

Culture of SiHa cells

The human cervical epithelial cell line, SiHa cells, was obtained from the American Type Culture Collection (ATCC, Manassas, Virginia, USA) and maintained in Dulbecco's Modified Eagle's Medium (DMEM) supplemented with 10% heat-inactivated fetal bovine serum (FBS; Gibco BRL, Grand Island, New York, USA) and antibiotic-antimycotic (Gibco BRL) in a 5% CO₂ atmosphere at 37°C.

T. vaginalis cultures

The *T. vaginalis* T016 strain was cultured according to previous papers [9, 14]. Briefly, *T. vaginalis* T016 isolate was cultured in glass, screw-capped tubes containing Diamond's trypticase yeast-extract maltose (TYM) medium (NAPCO, Winchester, VA, USA) supplemented with 10% heat-inactivated horse serum (Sigma-Aldrich, St Louis, MO, USA) in 5% CO₂ at 37°C for 24 h. The cultured parasites were monitored for motility, and their viability was determined before each experiment using trypan-blue staining (> 99%).

Experimental designs

SiHa cells were seeded on 96-well plates (for LDH and MTS assay), 12-well coverslips (for immunofluorescence and ROS detection), and 100-mm culture dishes (for western blotting) at various densities and grown to confluence at 37°C in 5% CO₂.

Live *T. vaginalis* trophozoites were incubated in SiHa cells using mixed-medium (DMEM/TYM = 2:1) at MOIs of 2 and 5 for 2 and 6 h or *T. vaginalis* MOI 5 for 6 h at 37°C in 5% CO₂. And then, the cytotoxicity, apoptosis, ROS production, MMP, induction of ER stress and its mechanism of action, and Bcl-2 family-

related protein expressions were evaluated in *T. vaginalis*-infected SiHa cells by MTS assay, LDH assay, flow cytometry, immunocytochemistry and western blotting.

To determine the role of ROS in *T. vaginalis*-infected cells, cells were pretreated with the ROS scavenger NAC, and then evaluated for apoptotic features, MMP and ER stress response. To assess the involvement of ER stress in apoptosis induction in *T. vaginalis*-infected SiHa cells, cells were pre-treated with ER stress inhibitor 4-PBA, NAC or the JNK inhibitor SP600125, and then the apoptotic features, ROS production, MMP, Bcl-2 family proteins and ASK1/JNK pathways were evaluated. Untreated SiHa cells were used as controls. Each experiment was performed at least three times in triplicate.

LDH Assay

The LDH assay was performed for cytotoxicity quantification with the CytoTox 96[®] Non-Radioactive Cytotoxicity Assay kit according to the manufacturer's protocol. Briefly, 1×10^4 cells were seeded in 96-well plates and infected with *T. vaginalis* at various MOI (2, 5) for the indicated times (0, 2, 6 h) in an incubator (5% CO₂, 90% relative humidity, 37°C). Then, 50 µL aliquots from all infected and control wells were transferred into a new 96-well plate, and 50 µL of CytoTox 96[®] reagent was added to each sample aliquot. The plate was covered with foil to protect the samples from light and incubated for 30 min at room temperature. After adding 50 µL of stop solution to each well, the absorbance of the solution was measured immediately at 490 nm using a microplate reader (TECAN, Crailsheim, Germany). LDH release levels in the media were quantified and compared to control values according to the kit instructions.

MTS Assay

The MTS assay was performed for detecting the cytotoxicity with the CellTiter 96[®] AQueous One Solution Cell Proliferation Assay kit according to the manufacturer's instruction. Briefly, 1×10^4 cells were seeded in 96-well plates and stimulated with various concentrations of NAC (0, 0.2, 1, 5 mM), 4-PBA (0, 0.2, 1, 5 mM), and SP600125 (0, 0.3, 3, 30 µM) for the indicated times (0, 2, 6, 12, 24 h) in an incubator (5% CO₂, 37°C). Following pipetting 20 µL of CellTiter 96[®] AQueous One Solution Reagent into each well of the 96-well assay plate containing the samples in 100 µL of culture medium, the samples were incubated at 37°C for 1–4 h in a humidified, 5% CO₂ atmosphere, and recorded the absorbance at 490 nm using a 96-well plate reader.

Measurement of ROS Generation by Confocal microscope

SiHa cells (1×10^5 cells/well; 12-well plate) seeded on a coverslip were cultured in DMEM supplemented with 10% FBS and the culture medium was replaced when the cells reached 80% confluence. To evaluate the generation of ROS, SiHa cells were infected with live *T. vaginalis* (MOI 2 and 5) for 2 h, and 6h, and then incubated with 5 µM MitoSOX reagent or CellROX reagent and then incubated for 10 min at 37°C, 5% CO₂ in the dark. The stained cells were imaged using an Olympus BX51 fluorescence microscope. All experiments were performed on triplicate samples and fluorescence intensity was calculated using ImageJ software, and graph was plotted using SigmaPlot 12.5 (Systat Software, San Jose, CA).

ROS-based Flow cytometric Assay

SiHa Cells were cultured in 12-well plates, and infected with *T. vaginalis* at MOI 2 and 5 for 0, 2 and 6 h with the indicated concentrations of NAC (0, 0.2, 1, 5 mM) pre-treatment or not. Followed by washing with PBS, the cells were removed from the well with 2.5% trypsin-EDTA and re-suspended in PBS with 5 μ M MitoSOX reagent or 5 μ M CellROX reagent and incubated at 37°C, protected from light, for 30 min. After gently three times washing, the cells were re-suspended in FACS buffer (1% BSA in PBS) and immediately subjected to the acquisition of 10,000 events with FACScan device (BD Biosciences, San Diego, CA, USA). The results are expressed as a histogram emitting the corresponding fluorescence, and as a bar graph representing the mean fluorescence intensity of all the groups.

Mitochondrial Membrane Potential (MMP) Assay

The MMP was measured using the JC-1 MitoMP detection kit (Dojindo, Kumamoto, Japan). Briefly, SiHa cells were seeded onto coverslips in 12-well plates at a density of 1×10^4 cells/well and infected with *T. vaginalis* at various conditions with or without specific inhibitors. The cells were then incubated with 4 μ M JC-1 fluorescence dye at 37°C for 30 min in dark and rinsed three times with HBSS. The stained cells were mounted onto microscope slides in VECTASHIELD HardSet Mounting Medium with DAPI (Vector Laboratories), and images were collected using a laser confocal microscope (Leica, TCS SP8, Wetzlar, Germany). The intensities of green (excitation/emission wavelength= 485/538 nm) and red (excitation/emission wavelength= 485/590 nm) fluorescence were analyzed for ≥ 6 microscopic fields in each sample.

Immunocytochemistry

SiHa cells were seeded onto coverslips in 12-well plates at a density of 1×10^4 cells/well and incubated for 24 h. The cells were pretreated with or without specific inhibitors for 2 h and then infected with *T. vaginalis* at MOI5 for 6 h. The cells were washed with HBSS and fixed with freshly prepared 4% paraformaldehyde for 1 h at room temperature. After washing three times with PBS containing 0.3% Triton X-100 (PBS-T) for 5 min, the cells were blocked with 1% BSA in 0.3% PBS-T for 30 min at room temperature and then incubated with CHOP primary antibody for 2 h at room temperature. The cells were washed to remove the excess primary antibody and then incubated with the appropriate fluorescently labeled secondary antibody (anti-mouse Alexa Fluor 647) for 2 h at room temperature. After mounting with VECTASHIELD HardSet antifade mounting medium with DAPI (Vector Laboratories, Burlingame, CA, USA) to stain the nucleus, fluorescence images were acquired using a Leica confocal software.

Western blotting analysis

SDS-PAGE and western blotting analysis were performed to determine numerous proteins expression. SiHa cells were cultured in 100-mm dishes and underwent serum deprivation for 4 h to remove stimulation from serum factors. Then cells were infected by *T. vaginalis* as indicated. After washing with PBS, proteins were extracted using the PRO-PREP Protein Extraction Solution (iNtRON Biotechnology,

Korea). The extract was incubated with the complete protease inhibitor cocktail (Roche, Basel, Switzerland) for 30 min on ice followed by boiling for 10 min, and then centrifuged at 14,000 g for 15 min at 4°C. The supernatant was collected, and equal amounts of protein from each sample were separated by SDS-PAGE and transferred to a polyvinylidene difluoride (PVDF) membrane (Bio-Rad Laboratories, Hercules, CA, USA). The membranes were immersed for blocking at 5% skim milk in Tris-buffered saline (20 mM Tris, 137 mM NaCl, pH 7.6) containing 0.1% Tween-20 (TBST) for 1 h at room temperature. After washing once in TBST, membranes were incubated overnight at 4°C with the primary antibodies diluted in TBST supplemented with 5% BSA. Following three consecutive washes with TBST, membranes were incubated for 90 min with HRP-conjugated anti-mouse or anti-rabbit secondary antibody diluted 1:2000 with 5% skim milk, as described above. The washed membranes were soaked with Immobilon Western Chemiluminescent HRP Substrate (Jackson ImmunoResearch Laboratories), and chemiluminescence was detected with a Fusion Solo System (Vilber Lourmat, Collégien, France). Band intensity was quantified using ImageJ software (NIH, Bethesda, MD, USA). These experiments were repeated at least three times.

Statistical analysis

All assays were performed in triplicate, and at least three independent experiments were conducted per test series. Results are presented as the means \pm standard deviation (SD). Statistical analysis of the data was performed using unpaired, two-tailed Student's t-tests. A P-value less than 0.05 indicated statistical significance.

Results

T. vaginalis induced cytotoxicity and apoptosis in SiHa cells in a parasite burden- and infection time-dependent manner

To assess the cytotoxicity of live *T. vaginalis* trophozoites in cervical epithelial SiHa cells, the cells were infected with *T. vaginalis* at different multiplicity of infection (MOI) and infection time before conducting the LDH assay. The cytotoxicity of SiHa cells infected with *T. vaginalis* at MOI 2 was $13.5 \pm 1.1\%$, $26.9 \pm 2.7\%$, and $46.9 \pm 1.7\%$ at 0, 2, and 6 h post-infection, respectively. Further, we observed that the toxicity of *T. vaginalis* in the SiHa cells was parasite burden-dependent, as it significantly increased to $48.9 \pm 2.8\%$ and $83.2 \pm 5.0\%$ at 2 and 6 h post-infection of *T. vaginalis* (MOI 5), respectively (Fig. 1A).

To determine whether this cytotoxicity was associated with apoptosis, we evaluated the apoptosis indicator proteins in the *T. vaginalis*-infected SiHa cells. The expression levels of cleaved PARP and caspase 3, as observed by western blotting, significantly increased from 2 h after *T. vaginalis* infection at MOI 2 in a parasite burden- and infection time-dependent manner (Fig. 1B).

Together, these results suggested that *T. vaginalis* induces cytotoxicity and apoptosis in SiHa cells in a parasite burden- and infection time-dependent manner.

T. vaginalis led to the generation of mitochondrial ROS in SiHa cells in parasite burden- and infection time-dependent manner

Oxidative stress is an important factor for cytotoxicity associated with apoptosis [17]. To investigate ROS production in *T. vaginalis*-infected SiHa cells, cellular and mitochondrial ROS levels were measured following infection. Cellular ROS levels significantly increased in the *T. vaginalis*-infected SiHa cells (MOI 2) from 2 h after infection and increased further at 6 h post-infection. Cellular ROS levels were significantly higher in the cells infected with *T. vaginalis* at MOI 5 than in cells infected with *T. vaginalis* at MOI 2 (Fig. 2A).

We further investigated mitochondrial ROS production using the MitoSOX Red staining technique and found that ROS production significantly increased from 2 h after *T. vaginalis* infection in direct proportion to parasite burden and infection time in the SiHa cells, which was similar to that in case of cellular ROS production (Fig. 2B).

These findings suggested that *T. vaginalis* induces mitochondrial ROS production in SiHa cells in a parasite burden- and infection time-dependent manner.

T. vaginalis induced mitochondrial apoptosis through ROS in SiHa cells

To determine whether ROS are involved in the induction of apoptosis in *T. vaginalis*-infected SiHa cells, the cells were pretreated with the ROS scavenger N-Acetyl cysteine (NAC) and the expression of apoptosis-related proteins and MMP was evaluated. We first determined the effects of NAC on cell viability using the MTS assay. Treatment of the SiHa cells with 0.2–1 mM NAC for 6 h elicited no significant differences in cell viability compared with those in the medium-treated group; however, the SiHa cells treated with 5 mM NAC for 6 h showed slightly reduced viability (see Additional file 1: Fig. S1A). Both cellular and mitochondrial ROS production were significantly suppressed in the *T. vaginalis*-infected SiHa cells following NAC pretreatment in a concentration-dependent manner (see Additional file 2: Fig. S2A, B).

As shown in Fig. 3A, in the NAC-pretreated SiHa cells, *T. vaginalis*-induced cleavage of PARP and caspase-3 was significantly suppressed in a dose-dependent manner. The permeabilization of the mitochondrial outer membrane is a crucial step in the progression of apoptosis [6, 7]; thus, we also investigated whether the *T. vaginalis*-induced ROS-dependent apoptosis in SiHa cells was related to the mitochondrial apoptotic pathways. JC-1 staining, an indicator of MMP. *T. vaginalis* infection, revealed a notable decrease in MMP levels, as indicated by the reduction in red fluorescence signal and an increase in green JC-1 fluorescence signal, in a parasite burden- and infection time-dependent manner compared

with the signals in untreated control cells (Fig. 3B). However, these changes in JC-1 dye fluorescence were suppressed by NAC pretreatment in a dose-dependent manner (Fig. 3C).

These results suggested that *T. vaginalis* induces mitochondrial apoptosis through ROS, and ROS act upstream of PARP and caspase-3 during apoptosis induction.

***T. vaginalis* induced ER stress response and ER stress-mediated apoptosis in SiHa cells.**

ER stress is known to contribute to apoptosis [18, 19, 21]. First, to check whether *T. vaginalis* causes ER stress in SiHa cells, we investigated the expression of ER stress-related proteins in *T. vaginalis*-infected SiHa cells. As shown in Fig. 4A, Ero1-La, p-IRE1α, CHOP, p-PERK, p-eIF2α, ATF4, and cleaved ATF6 protein levels were significantly increased in the *T. vaginalis*-infected SiHa cells in a parasite burden- and infection time-dependent manner, whereas procaspase-12 levels were decreased as compared with those in the untreated control group (Fig. 4A).

Next, to confirm whether apoptosis is induced by ER stress in *T. vaginalis*-infected SiHa cells, the cells were pretreated with the ER stress inhibitor 4-phenylbutyric acid (4-PBA), and the expression of ER stress- and apoptosis-related proteins was evaluated. The SiHa cells treated with 5 mM 4-PBA for 6 h did not show a significant difference in viability compared with that of the untreated control group (see Additional file 1: Fig. S1B). The expression of ER stress-related proteins was reversed in the 4-PBA-pretreated *T. vaginalis*-infected SiHa cells in a dose-dependent manner as compared with that in the untreated *T. vaginalis*-infected cells (Fig. 4B). In addition, 4-PBA pretreatment attenuated the levels of cleaved PARP and caspase-3 in *T. vaginalis*-infected SiHa cells in a dose-dependent manner (Fig. 4C). These results demonstrated that *T. vaginalis* induces ER stress response as well as ER stress-mediated apoptosis in SiHa cells.

***T. vaginalis* induced ROS-dependent ER stress responses in SiHa cells.**

ER and mitochondria are closely related, both structurally and functionally [18, 19, 22, 23]. Thus, to evaluate the effects of mitochondrial ROS in the induction of ER stress response in *T. vaginalis*-infected SiHa cells, the SiHa cells were pretreated with NAC, and the expression of ER stress-related proteins was investigated. Pretreatment with NAC significantly reduced the expression of Ero1-La, p-IRE1α, CHOP, p-PERK, p-eIF2α, ATF4, and cleaved ATF6 in the *T. vaginalis*-infected SiHa cells in a dose-dependent manner, whereas the expression level of procaspase-12 was increased in a dose-dependent manner (Fig. 5A). Confocal microscopy imaging also confirmed that NAC pretreatment reduced *T. vaginalis*-induced upregulation of CHOP protein expression in a dose-dependent manner (Fig. 5B).

These results indicated that *T. vaginalis* induces ER stress response through mitochondrial ROS in SiHa cells, which leads to apoptosis.

***T. vaginalis* induced ER stress-mediated mitochondrial dysfunction in SiHa cells.**

We also investigated whether ER stress affects mitochondrial functions in *T. vaginalis*-infected SiHa cells. Members of the Bcl-2 family are major regulators of mitochondrial integrity and mitochondria-dependent caspase activation, and MMP is the key indicator of mitochondrial apoptosis [6, 7]. Therefore, we investigated mitochondrial functions, including alternation of MMP and Bcl-2 family members, in *T. vaginalis*-infected SiHa cells. JC-1 dye staining revealed that *T. vaginalis* induced MMP depolarization in the SiHa cells; however, these changes in fluorescence were suppressed by 4-PBA pretreatment (Fig. 6A).

The expression of p-Bad (Ser112), Bax, Bak, Bik, and Puma was significantly increased in the *T. vaginalis*-infected SiHa cells (Fig. 6B), whereas the Bcl-xL and Mcl-1 levels were decreased in a parasite burden-dependent manner (Fig. 6C). The expression levels of p-Bad (Ser 112), Bax, Bak, Bik, and Puma were significantly decreased in the 4-PBA-pretreated *T. vaginalis*-infected SiHa cells in a dose-dependent manner (Fig. 6D), whereas the levels of Bcl-xL and Mcl-1 proteins were increased (Fig. 6E). These results clearly indicated that *T. vaginalis* induces mitochondrial dysfunction via ER stress in SiHa cells, leading to apoptosis.

***T. vaginalis* induced ER stress-mediated mitochondrial apoptosis via the IRE1/ASK1/JNK/Bcl-2 family protein pathways in SiHa cells.**

Previous studies have reported that the IRE1/ASK1/JNK signaling cascade is one of the main downstream targets for the regulation of ER stress-induced cell apoptosis [18, 19, 21–23]. Therefore, we investigated whether *T. vaginalis* activates ER stress-dependent apoptosis through the ASK1/JNK pathway in SiHa cells. We found a substantial increase in the phosphorylation levels of both ASK1 (Ser83, Ser967, and Thr845) and JNK in the *T. vaginalis*-infected SiHa cells in a parasite burden- and infection time-dependent manner (Fig. 7A). Next, we investigated whether ASK1/JNK activation was related to ER stress in the *T. vaginalis*-infected SiHa cells. Western blotting analysis revealed that 4-PBA pretreatment attenuated the *T. vaginalis*-induced elevation of ASK1 and JNK phosphorylation levels in a dose-dependent manner (Fig. 7B). These data indicated that the *T. vaginalis*-induced ER stress activates the ASK1/JNK pathway in SiHa cells.

To evaluate whether the ASK1/JNK pathway is associated with mitochondrial apoptosis in *T. vaginalis*-infected SiHa cells, the cells were preincubated with the JNK inhibitor SP600125, and expression of MMP, Bcl-2 family proteins, and apoptosis-related proteins was investigated. The SiHa cells treated with 30 μ M

SP600125 for 6 h did not display a significant difference in their viability as compared with those of the untreated control group (see Additional file 1: Fig. S1C). Western blotting analysis revealed that Bak, Bax, cleaved PARP, and caspase-3 levels decreased in a dose-dependent manner in the SP600125-pretreated *T. vaginalis*-infected SiHa cells (Fig. 7C). In contrast, Bcl-xL and Mcl-1 levels were increased by pretreatment with SP600125 in the *T. vaginalis*-infected SiHa cells in a dose-dependent manner (Fig. 7D). In addition, SP600125 pretreatment substantially increased MMP levels in the *T. vaginalis*-infected SiHa cells, as demonstrated by increased red and reduced green JC-1 fluorescence, in a dose-dependent manner (Fig. 7E). These observations provided evidence that *T. vaginalis* induces ER stress-mediated mitochondrial apoptosis via the IRE1/ASK1/JNK/Bcl-2 family protein signaling pathways in SiHa cells.

Discussion

Trichomoniasis is a highly prevalent STI; however, its pathophysiology remains unclear. In this study, we evaluated the role of ER stress in apoptosis induction in *T. vaginalis*-infected human cervical epithelial SiHa cells. We observed that *T. vaginalis* induces apoptosis through mitochondrial ROS production associated with mitochondrial dysfunction and ER stress response in a parasite burden- and infection time-dependent manner. Also *T. vaginalis* induces ROS-dependent ER stress response and ER stress-mediated mitochondrial apoptosis in SiHa cells. To the best of our knowledge, this is the first study on ER stress involvement in apoptosis induction of *T. vaginalis*-infected mammalian cells via the ROS-ER stress-mitochondrial apoptosis pathways.

ROS generation is one of the most critical factors for apoptosis induction in *T. vaginalis*-infected mammalian cells [8, 9]. The present findings showed that *T. vaginalis* induces mitochondrial ROS production in SiHa cells in a parasite burden- and infection time-dependent manner, and also induces apoptosis and ER stress response. Thus, we investigated the effects of ROS on ER stress induction in *T. vaginalis*-infected SiHa cells. Perturbations in the physiological status of the ER trigger a specific response known as the ER stress response or unfolded protein response (UPR), which induces premature apoptosis [18, 19, 21]. ROS induce ER stress-mediated apoptosis during some viral and bacterial infections [24–26]. Previous studies have shown that ER stress induces apoptosis of cells infected with *Mycobacterium* [24], *Toxoplasma* [28], *Leishmania* [29], etc. In mammalian cells, ER stress signaling is typically sensed by three major ER-resident transmembrane molecules—IRE1, PERK, and ATF6 [18, 21, 27]. In this study, *T. vaginalis* infection upregulated p-IRE1α, p-PERK, ATF4, cleaved ATF6, and CHOP levels and downregulated the levels of procaspase-4 and -12 in SiHa cells in a parasite burden- and infection time-dependent manner. However, 4-PBA and NAC pretreatment significantly reversed the expression of ER stress-related proteins in *T. vaginalis*-infected SiHa cells in a dose-dependent manner. Our results indicated that *T. vaginalis* induces a direct ER stress response as well as via an ROS-dependent ER stress response in SiHa cells. Furthermore, 4-PBA or NAC pretreatment apparently suppressed the apoptosis and mitochondrial ROS production in *T. vaginalis*-infected SiHa cells. These results indicated that *T. vaginalis* induces ER stress-mediated apoptosis in SiHa cells besides ROS-dependent apoptosis; thus, ER stress is responsible for apoptosis induction in *T. vaginalis*-infected SiHa cells. ER stress-mediated apoptosis has

also been observed in *T. gondii*-infected neural cells [28] and *Leishmania infantum*-infected macrophages [29].

ER and mitochondria communicate with each other *via* calcium and ROS [18, 19, 22]. Mitochondria are important in the regulation and transmission of apoptotic signals, which are regulated by a balance between the Bcl-2-family proteins [7, 22]. In our study, *T. vaginalis* induced MMP depolarization, which led to an increase in Bak and Bax levels and a decrease in Bcl-xL and Mcl-1 levels; this caused mitochondrial dysfunction, which could have stimulated the release of cytochrome c into the cytosol of the *T. vaginalis*-infected cells [12–14]. However, pretreatment with NAC or 4-PBA effectively reversed MMP depolarization and the expression pattern of Bcl-2 family proteins in a dose-dependent manner. These data suggested that *T. vaginalis* induces mitochondrial apoptosis in SiHa cells through ROS as well as *T. vaginalis*-induced ER stress. These findings are in accordance with those reported in previous studies, wherein *M. avium* induced apoptosis through ROS-dependent ER stress response in macrophages [24] and silibinin, a biologically active compound of milk thistle, induced mitochondrial ROS-dependent apoptosis through ER stress response and disruption of Ca²⁺ homeostasis in prostate cell lines [30].

The apoptotic crosstalk between the ER and the mitochondria is regulated by Bcl-2 family proteins, and ER stress regulates the expression of the Bcl-2 family proteins, ultimately leading to the mitochondria-mediated apoptotic caspase cascade [18, 19, 22, 23]. During severe and sustained ER stress conditions, the intrinsic apoptotic pathway can be activated by IRE1-mediated activation of tumor necrosis factor receptor-associated factor 2 (TRAF2), which stimulates the ASK1/JNK kinase cascade [21, 25, 27]. Thus, we investigated the involvement of the IRE1/ASK1/JNK pathways during ER stress-induced apoptosis and found that *T. vaginalis* induced ASK1 and JNK phosphorylation in SiHa cells. However, pretreatment with 4-PBA or SP600125 attenuated the expression levels of IRE1α, cleaved caspase-3 and PARP, p-ASK1, and p-JNK in the *T. vaginalis*-infected SiHa cells. In addition, we investigated the involvement of Bcl-2 family members, which act downstream of the IRE1/ASK1/JNK pathways, during ER stress-induced apoptosis. Pretreatment with 4-PBA or SP600125 increased the expression of MMP, Bcl-xL, and Mcl-1, whereas attenuated the expression of Bax and Bak in the *T. vaginalis*-infected SiHa cells in a dose-dependent manner. These results indicated that ER stress and Bcl-2 family proteins communicate with each other during apoptosis induction, and *T. vaginalis* induces apoptosis via ER stress-mediated mitochondrial dysfunction in SiHa cells through the IRE1/ASK1/JNK apoptotic pathways. These findings could be explained by previous reports suggesting that Bax and Bak localize to both the mitochondria and ER and their over-expression promotes apoptotic calcium mobilization during ER-mediated mitochondrial cell death [31, 32]. A similar apoptotic mechanism was reported in silica nanoparticle-treated endothelial cells, wherein apoptosis was induced through the ER stress-associated IRE1/JNK, CHOP, and caspase-12 down to the mitochondria via Bcl-2 family members [33].

Conclusions

Our results showed that *T. vaginalis* induced apoptosis through mitochondrial ROS generation and ER stress response as well as induced direct and ROS-dependent ER stress response in SiHa cells. *T.*

vaginalis also induced ER stress-mediated mitochondrial dysfunction and finally led to apoptosis of SiHa cells through the IRE1/ASK1/JNK/Bcl-2 family protein pathways (Fig. 8). Thus, *T. vaginalis* infection induces apoptosis via ROS-ER stress-mitochondrial apoptosis pathways by interacting with the mitochondria and ER in human cervical epithelial SiHa cells. These findings may contribute to expand our understanding of the molecular mechanisms underlying the pathogenesis of human trichomoniasis.

Abbreviations

ASK1: apoptosis signal regulating kinase 1; ATF: activating transcription factor; CHOP: CCAAT/enhancer-binding protein–homologous protein; DAPI: 4',6-diamidino-2-phenylindole; ER: endoplasmic reticulum; IRE1: inositol-requiring enzyme 1; JC-1: 5,5',6,6'-Tetrachloro-1,1',3,3'-tetraethyl-imidacarbocyanine iodide; JNK: c-Jun N-terminal kinases; LDH: lactate dehydrogenase; MMP: mitochondrial membrane potential; MOI: multiplicities of infection; NAC: *N*-Acetyl cysteine; PARP poly(ADP-ribose) polymerase; 4-PBA: 4-phenylbutyric acid; PERK: protein kinase RNA-like ER kinase; SD: standard deviation; TRAF2: tumor necrosis factor receptor-associated factor 2.

Declarations

Availability of data and materials

All datasets generated during the present study are included in the published article including Additional files.

Acknowledgements

Not applicable.

Funding

This work was supported by Basic Science Research Program through the National Research Foundation of Korea (NRF) funded by the Ministry of Science, ICT and Future Planning (NRF-2019R1A2C1088346) at Chungnam National University, and the National Natural Science Foundation of China (81971389 and 81771612), the Science Foundation of Guangdong Medical University (GDMUZ201801), the Natural Science Foundation of Guangdong Province (2019A1515011888 and 2019A1515011715).

Author information

¹Brain Korea 21 FOUR Project for Medical Science, Chungnam National University, Daejeon 35015, Republic of Korea: Fei Fei Gao, Jae-Min Yuk & Young-Ha Lee

²Department of Medical Science and Department of Infection Biology, Chungnam National University, Daejeon 35015, Republic of Korea: Fei Fei Gao, Jae-Min Yuk, Guang-Ho Cha & Young-Ha Lee

³Department of Gastroenterology, Affiliated Hospital of Guangdong Medical University, Zhanjiang, Guangdong Province 524001, China: Juan-Hua Quan

⁴Department of Obstetrics and Gynecology, Chungnam National University, Deajeon 35015, Korea: Min A Lee

⁵Department of Obstetrics and Gynecology, The Affiliated Hospital of Guangdong Medical University, Zhanjiang, Guangdong 524001, China: Wei Ye

Authors' contributions

FFG, JHQ, MAL and YHL designed and conceived the experiments. FFG, JHQ, MAL, WY, JMK, GHC, IWC and YHL carried out the experiments. FFG, JHQ, MAL, WY, JMK, GHC, IWC and YHL performed the data analysis. FFG, JHQ, MAL and YHL drafted and revised the manuscript. All authors read and approved the final manuscript.

Ethics approval and consent to participate

Not applicable.

Consent for publication

Not applicable.

Competing interests

The authors declare that they have no competing interests.

References

1. Kissinger P. Epidemiology and Treatment of Trichomoniasis. *Curr Infect Dis Rep.* 2015;17:484.
2. Rowley J, Vander Hoorn S, Korenromp E, Low N, Unemo M, Abu-Raddad LJ, et al. *Chlamydia, gonorrhoea, trichomoniasis and syphilis: Global prevalence and incidence estimates, 2016.* Bull World Health Organ. 2019;97:548–562.
3. Hosny AEMS, El-Khayat W, Kashef MT, Fakhry MN. Association between preterm labor and genitourinary tract infections caused by *Trichomonas vaginalis*, *Mycoplasma hominis*, Gram-

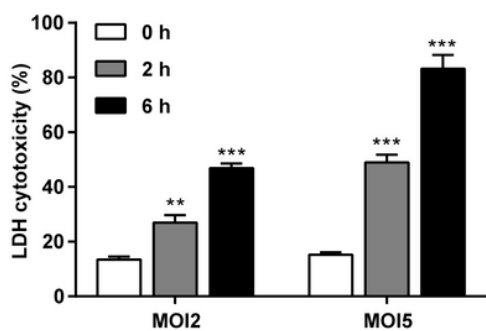
negative bacilli, and coryneforms. J Chin Med Assoc. 2017;80:575-581.

4. Yang S, Zhao W, Wang H, Wang Y, Li J, Wu X. *Trichomonas vaginalis* infection-associated risk of cervical cancer: A meta-analysis. Eur J Obstet Gynecol Reprod Biol. 2018;228:166-173.
5. Shafir SC, Sorvillo FJ, Smith L. Current issues and considerations regarding trichomoniasis and human immunodeficiency virus in African-Americans. Clin Microbiol Rev. 2009;22:37–45.
6. Zimmermann KC, Green DR. How cells die: apoptosis pathways. J Allergy Clin Immunol. 2001;108:99-103.
7. Bhola PD, Letai A. Mitochondria-Judges and Executioners of Cell Death Sentences. Mol Cell. 2016;61:695-704.
8. Song HO, Shin MH, Ahn MH, Min DY, Kim YS, Ryu JS. *Trichomonas vaginalis*: Reactive oxygen species mediates caspase-3 dependent apoptosis of human neutrophils. Exp Parasitol. 2008;118:59-65.
9. Quan JH, Kang BH, Yang JB, Rhee YE, Noh HT, Choi IW, et al. *Trichomonas vaginalis* Induces SiHa Cell Apoptosis by NF-kappaB Inactivation via Reactive Oxygen Species. Biomed Res Int. 2017;2017:3904870.
10. Sommer U, Costello CE, Hayes GR, Beach DH, Gilbert RO, Lucas JJ, et al. Identification of *Trichomonas vaginalis* cysteine proteases that induce apoptosis in human vaginal epithelial cells. J Biol Chem. 2005;280:23853-23860.
11. Kummer S, Hayes GR, Gilbert RO, Beach DH, Lucas JJ, Singh BN. Induction of human host cell apoptosis by *Trichomonas vaginalis* cysteine proteases is modulated by parasite exposure to iron. Microb Pathog. 2008;44:197-203.
12. Quan JH, Kang BH, Cha GH, Zhou W, Koh YB, Yang JB, et al. *Trichomonas vaginalis* metalloproteinase induces apoptosis of SiHa cells through disrupting the Mcl-1/Bim and Bcl-xL/Bim complexes. PLoS One. 2014;9:e110659.
13. Zhu Z, Zhao L, Brittingham A, Bai Q, Wakefield MR, Fang Y. *Trichomonas vaginalis* Inhibits HeLa Cell Growth Through Modulation of Critical Molecules for Cell Proliferation and Apoptosis. Anticancer Res. 2018;38:5079-5086.
14. Kang JH, Song HO, Ryu JS, Shin MH, Kim JM, Cho YS, et al. *Trichomonas vaginalis* promotes apoptosis of human neutrophils by activating caspase-3 and reducing Mcl-1 expression. Parasite Immunol. 2006;28:439–446.
15. Song HO, Lim YS, Moon SJ, Ahn MH, Ryu JS. Delayed human neutrophil apoptosis by *Trichomonas vaginalis* lysate. Korean J Parasitol. 2010;48:1-7.
16. Chang JH, Kim SK, Choi IH, Lee SK, Morio T, Chang EJ. Apoptosis of macrophages induced by *Trichomonas vaginalis* through the phosphorylation of p38 mitogen- activated protein kinase that locates at downstream of mitochondria-dependent caspase activation. Int J Biochem Cell Biol. 2006;38:638-647.
17. Dunn JD, Alvarez LA, Zhang X, Soldati T. Reactive oxygen species and mitochondria: A nexus of cellular homeostasis. Redox Biol. 2015;6:472–485.

18. Bravo-Sagua R, Rodriguez AE, Kuzmicic J, Gutierrez T, Lopez-Crisosto C, Quiroga C, et al. Cell death and survival through the endoplasmic reticulum-mitochondrial axis. *Curr Mol Med*. 2013;13:317–329.
19. Gutiérrez T, Simmen T. Endoplasmic reticulum chaperones tweak the mitochondrial calcium rheostat to control metabolism and cell death. *Cell Calcium*. 2018;70:64-75.
20. Gu NY, Kim JH, Han IH, Im SJ, Seo MY, Chung YH, et al. *Trichomonas vaginalis* induces IL-1beta production in a human prostate epithelial cell line by activating the NLRP3 inflammasome via reactive oxygen species and potassium ion efflux. *Prostate*. 2016;76:885-96.
21. Sano R, Reed JC. ER stress-induced cell death mechanisms. *Biochim Biophys Acta*. 2013;1833:3460-3470.
22. Su J, Zhou L, Xia MH, Xu Y, Xiang XY, Sun LK. Bcl-2 family proteins are involved in the signal crosstalk between endoplasmic reticulum stress and mitochondrial dysfunction in tumor chemotherapy resistance. *Biomed Res Int*. 2014;2014:234370.
23. Smith JA. STING, the Endoplasmic Reticulum, and Mitochondria: Is Three a Crowd or a Conversation? *Front Immunol*. 2021;11:611347.
24. Go D, Lee J, Choi JA, Cho SN, Kim SH, Son SH, et al. Reactive oxygen species-mediated endoplasmic reticulum stress response induces apoptosis of *Mycobacterium avium*-infected macrophages by activating regulated IRE1-dependent decay pathway. *Cell Microbiol*. 2019;21:e13094.
25. Pillich H, Loose M, Zimmer KP, Chakraborty T. Diverse roles of endoplasmic reticulum stress sensors in bacterial infection. *Mol Cell Pediatr*. 2016;3:9.
26. Jheng JR, Ho JY, Horng JT. ER stress, autophagy, and RNA viruses. *Front Microbiol*. 2014;5:388.
27. Galluzzi L, Diotallevi A, Magnani M. Endoplasmic reticulum stress and unfolded protein response in infection by intracellular parasites. *Future Sci OA*. 2017;3:FS0198.
28. Wan L, Gong L, Wang W, An R, Zheng M, Jiang Z, et al. *T. gondii* rhoptry protein ROP18 induces apoptosis of neural cells via endoplasmic reticulum stress pathway. *Parasit Vectors*. 2015;8:554.
29. Galluzzi L, Diotallevi A, De Santi M, Ceccarelli M, Vitale F, Brandi G, et al. *Leishmania infantum* Induces Mild Unfolded Protein Response in Infected Macrophages. *PLoS One*. 2016;11:e0168339.
30. Kim SH, Kim KY, Yu SN, Seo YK, Chun SS, Yu HS, et al. Silibinin induces mitochondrial NOX4-mediated endoplasmic reticulum stress response and its subsequent apoptosis. *BMC Cancer*. 2016;16:452.
31. Nutt LK, Pataer A, Pahler J, Fang B, Roth J, McConkey DJ, et al. Bax and Bak promote apoptosis by modulating endoplasmic reticular and mitochondrial Ca²⁺ stores. *J Biol Chem*. 2002;277:9219–9225.
32. Klee M, Pallauf K, Alcala S, Fleischer A, Pimentel-Muiños FX. Mitochondrial apoptosis induced by BH3-only molecules in the exclusive presence of endoplasmic reticular Bak. *EMBO J*. 2009;28:1757–1768.

Figures

A



B

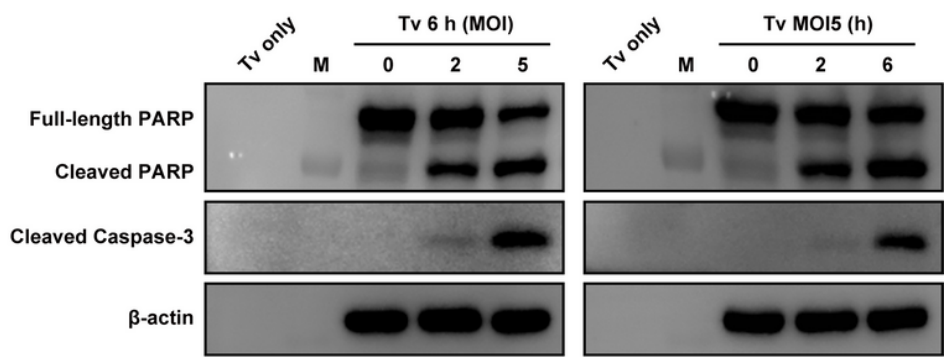
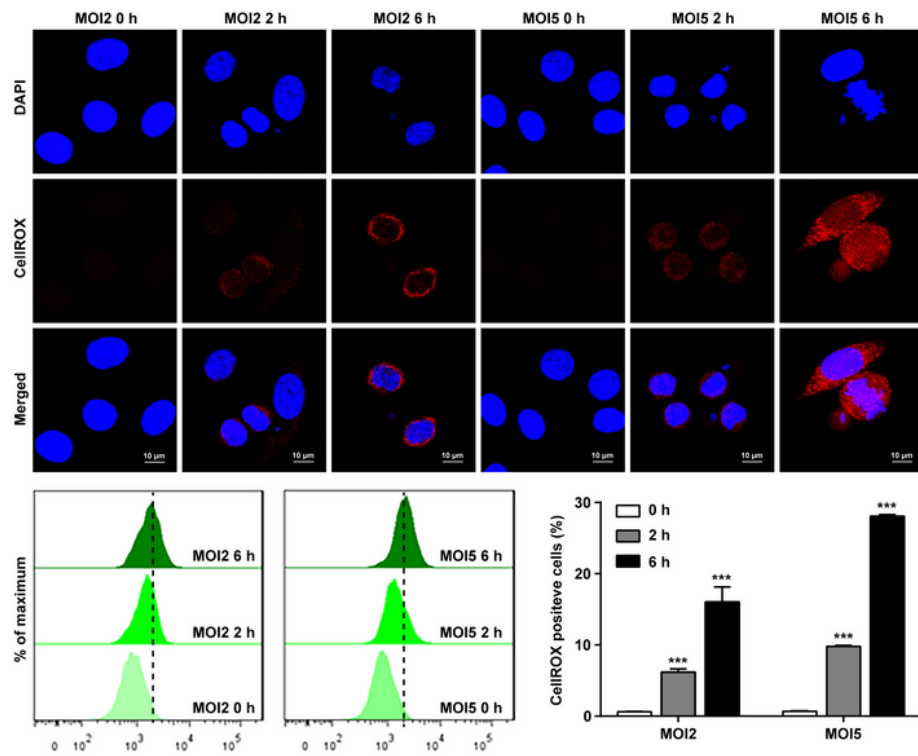
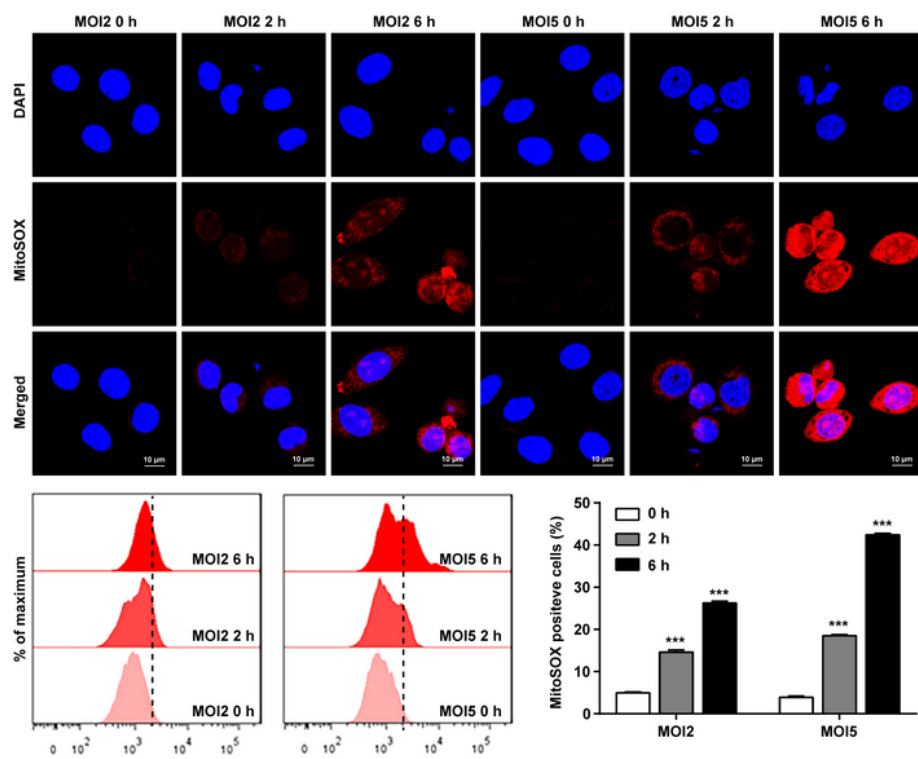


Figure 1

Trichomonas vaginalis induced cytotoxicity and apoptosis in cervical epithelial SiHa cells. SiHa cells were infected with live *T. vaginalis* trophozoites at MOI 2 and 5 for 0, 2, or 6 h. (A) The lactate dehydrogenase (LDH) level in the medium, which is related to cell death, was measured by LDH assay at indicated conditions. The data represent the mean value \pm standard deviations (SD) of at least three independent experiments. **P<0.01, ***P<0.001, compared with untreated control cells under the same conditions. (B) Cleaved PARP and caspase-3 protein levels were assessed using western blotting analysis. Anti-β-actin was used as an internal control. The data shown are representative of three independent experiments with similar results.

A**B****Figure 2**

T. vaginalis induced mitochondrial ROS production in SiHa cells. (A) Cellular ROS production was determined by the CellROX, a fluorogenic probe for measuring oxidative stress in live cells. Plots depict the CellROX positive cells as determined by densitometric analysis of flow cytometry. (B) Mitochondrial ROS production was determined by confocal microscopy and flow cytometry with MitoSOX, a mitochondrial ROS dye. Plots depict the MitoSOX positive cells as determined by densitometric analysis

of flow cytometry. Data shown are representative of three independent experiments with similar results.

***P<0.001, compared with the untreated control cells under the same conditions

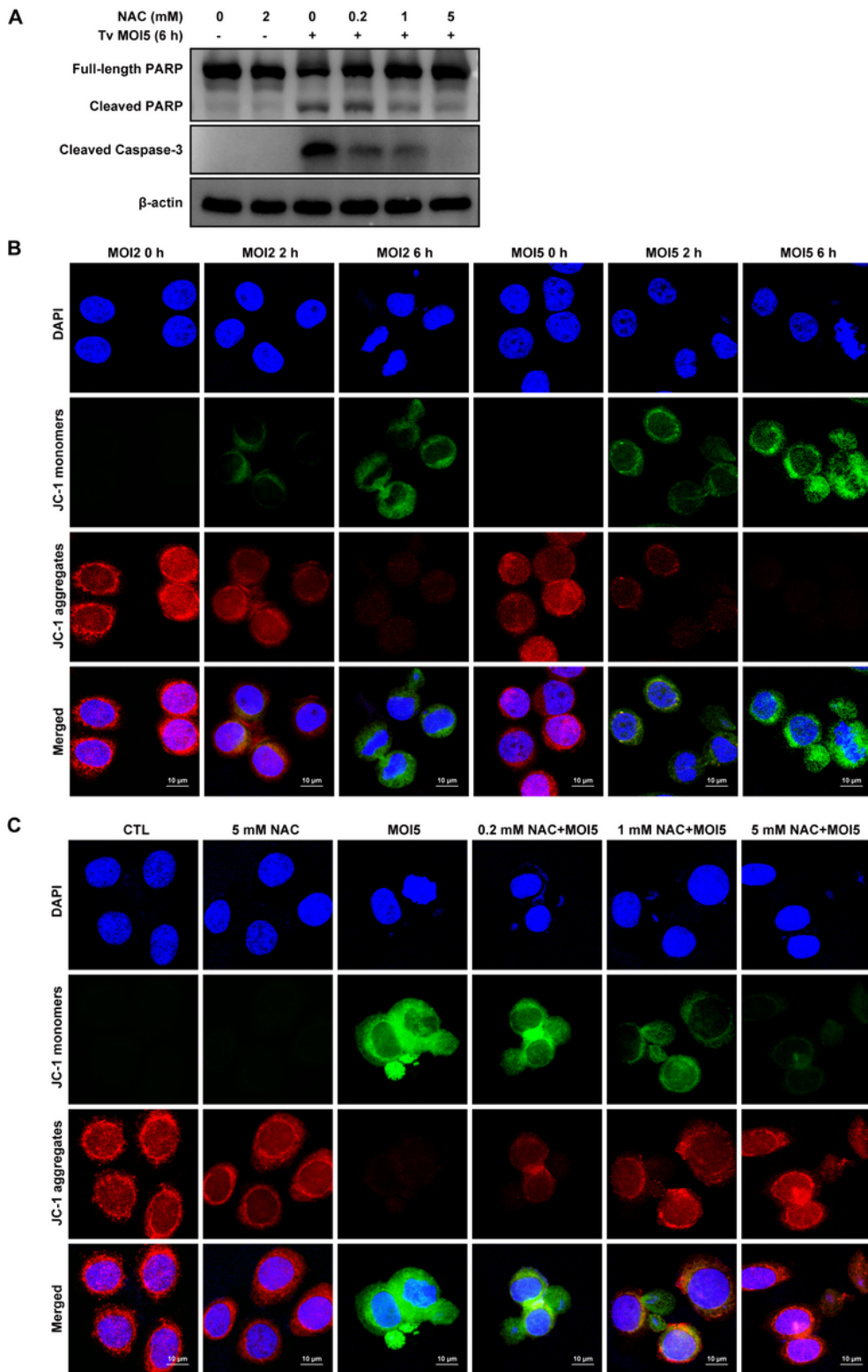
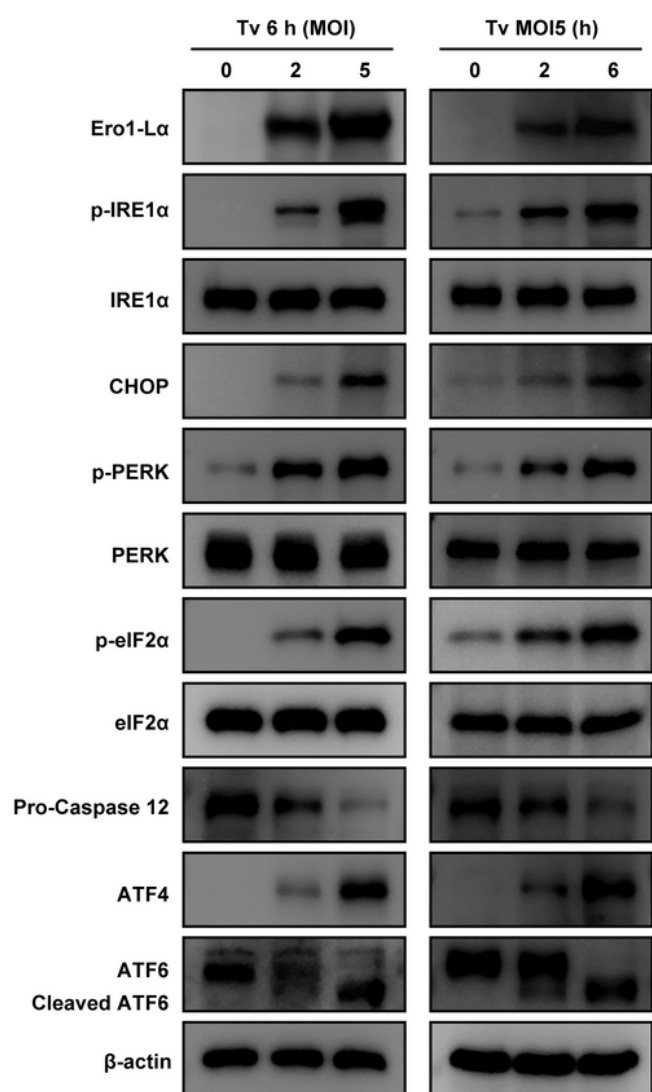


Figure 3

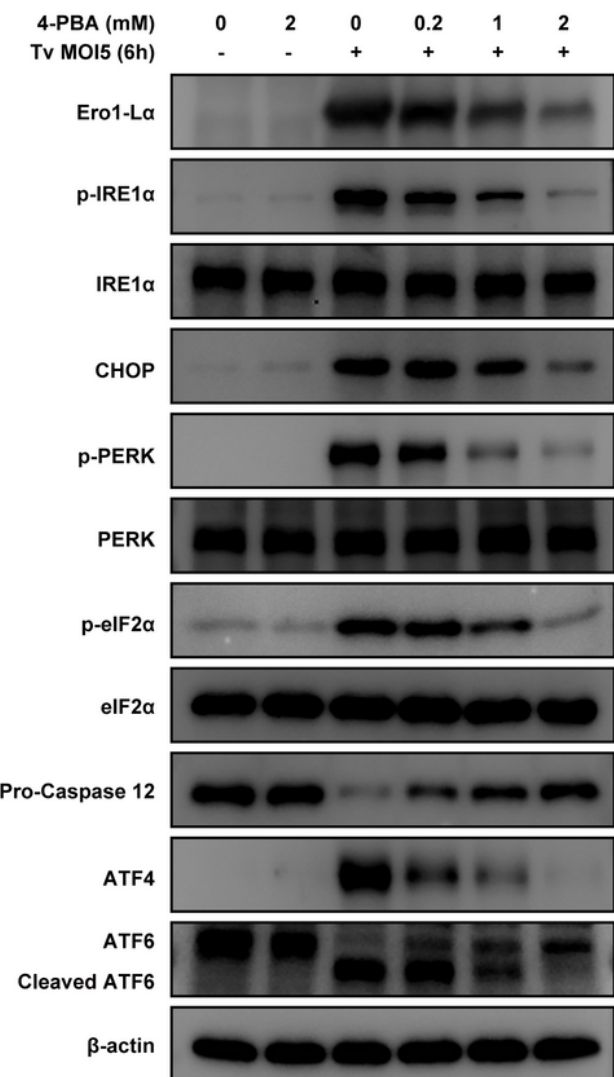
T. vaginalis induced mitochondrial apoptosis through ROS in SiHa cells. (A) SiHa cells were pretreated with various concentrations of an ROS scavenger (N-Acetyl cysteine: NAC) for 2 h, and subsequently infected with *T. vaginalis* at MOI 5 for 6 h. Cleaved PARP and caspase 3 protein levels were assessed by

western blotting. (B) SiHa cells were infected with *T. vaginalis* under the indicated conditions, and JC-1 staining was observed by confocal fluorescence microscopy. In JC-1–stained cells, red fluorescence is visible in cells with high mitochondrial membrane potential, while green fluorescence of JC-1 monomer is present in cells with low mitochondrial potential. (C) SiHa cells were pretreated with various concentration of NAC for 2 h, and subsequently infected with *T. vaginalis* at MOI 5 for 6 h. JC-1 staining was observed using confocal fluorescence microscopy. Data shown are representative of three independent experiments with similar results.

A



B



C

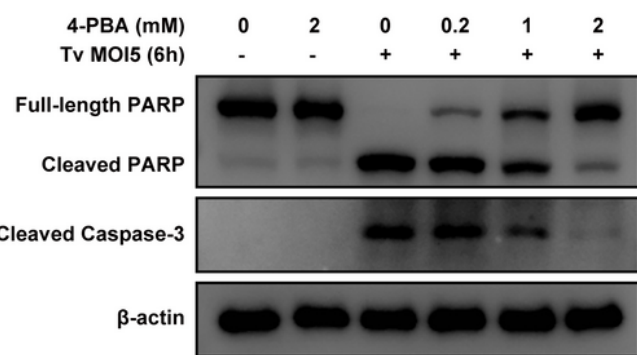
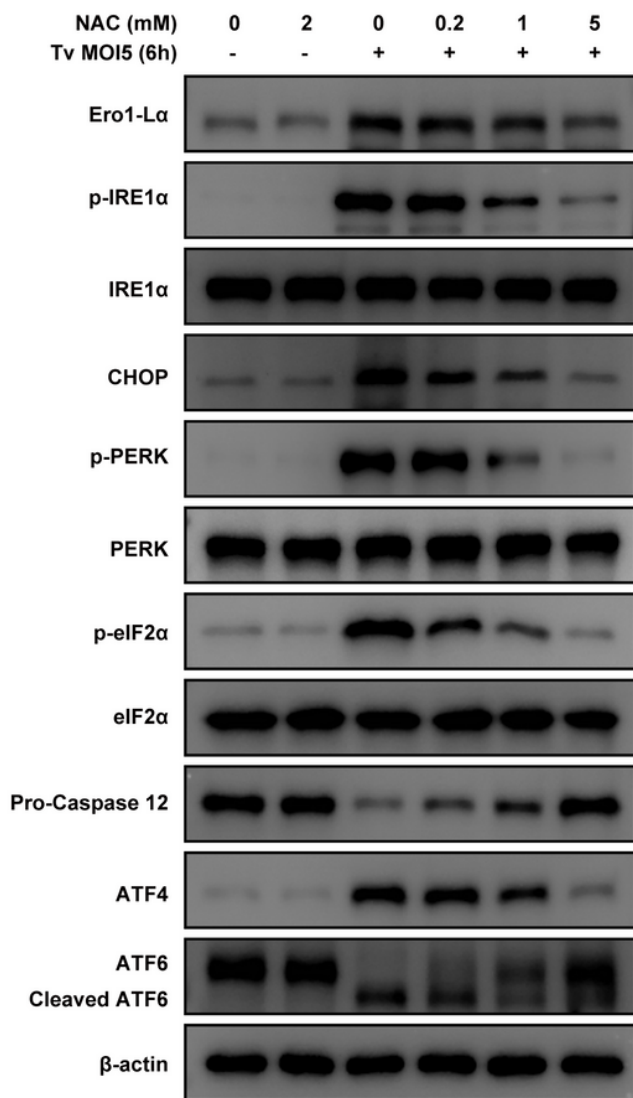


Figure 4

T. vaginalis induced ER stress response and ER stress-dependent apoptosis in SiHa cells. (A) SiHa cells were infected with *T. vaginalis* under the indicated conditions, and ER stress-related proteins were evaluated by western blotting analysis. (B, C) SiHa cells were pretreated with various concentrations of an ER stress inhibitor (4-phenylbutyrate: 4-PBA) for 2 h, and subsequently infected with *T. vaginalis* at MOI 5 for 6 h. The ER stress-related (B) and apoptosis-related (C) protein levels were assessed using western blotting analysis. Anti- β -actin was used as an internal control. The data shown are representative of three independent experiments with similar results.

A



B

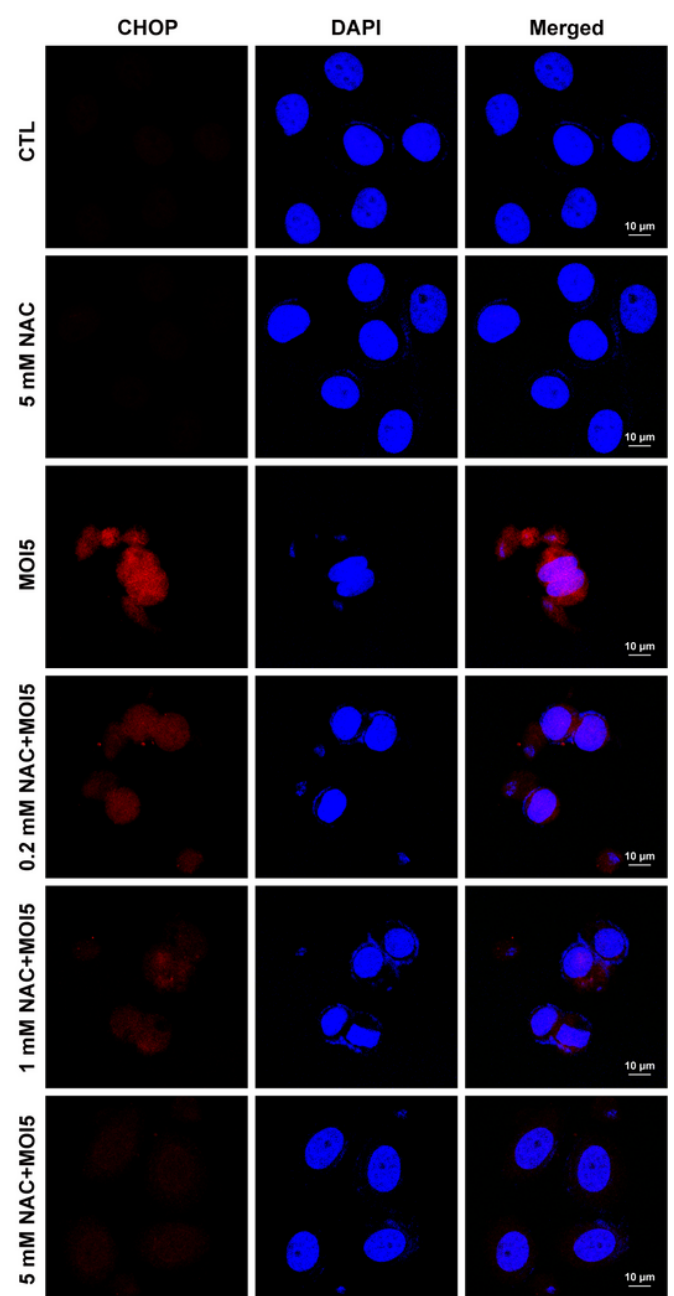


Figure 5

T. vaginalis-induced ROS-dependent ER stress response in SiHa cells. SiHa cells were pretreated with various concentrations of NAC for 2 h, and subsequently infected with *T. vaginalis* at MOI 5 for 6 h. (A) The ER stress-related protein levels were assessed using western blotting analysis. Anti- β -actin was used as an internal control. (B) Representative images obtained by confocal fluorescence microscopy stained with CHOP antibody. The data shown are representative of three independent experiments with similar results.

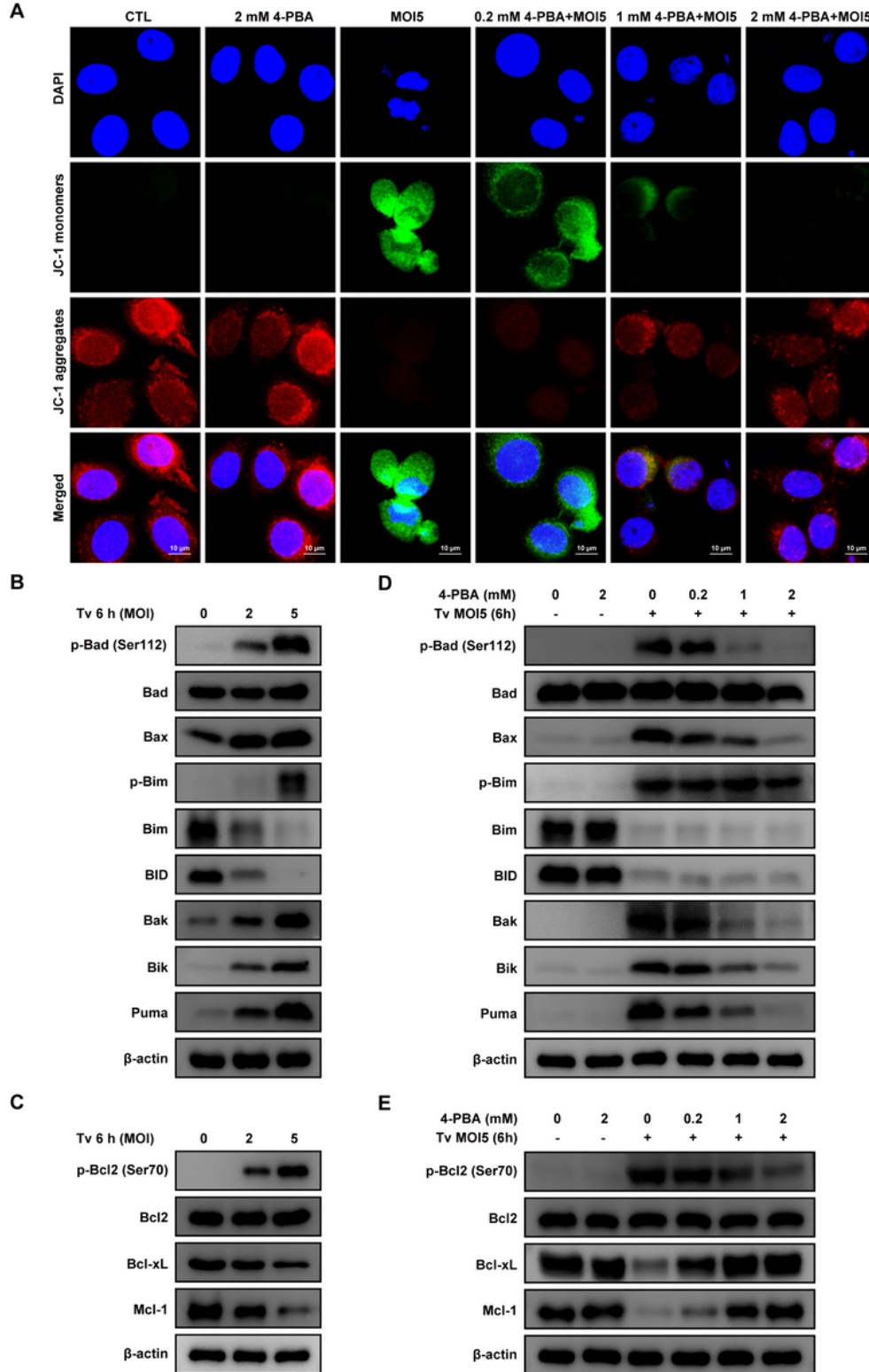


Figure 6

T. vaginalis induced ER stress-dependent mitochondrial dysfunction in SiHa cells. (A) SiHa cells were pretreated with various concentrations of 4-PBA for 2 h, and subsequently infected with *T. vaginalis* at MOI 5 for 6 h. SiHa cells were stained with JC-1 and fluorescence detected under a confocal microscope. The figure shows representative confocal images of JC-1 aggregate (red) and monomer (green) fluorescence, respectively. (B, C) SiHa cells were infected with *T. vaginalis* at MOI 2 and 5 for 6 h. Pro-apoptosis Bcl-2 (B) and Pro-Survival Bcl-2 (C) family members were evaluated by western blotting. (D, E) SiHa cells were pretreated with various concentrations of 4-PBA for 2 h, and subsequently infected with *T. vaginalis* at MOI 5 for 6 h. Pro-apoptosis Bcl2 (D) and Pro-Survival Bcl-2 (E) family members were evaluated by western blotting. Anti- β -actin was used as internal control. The data shown are representative of three independent experiments with similar results.

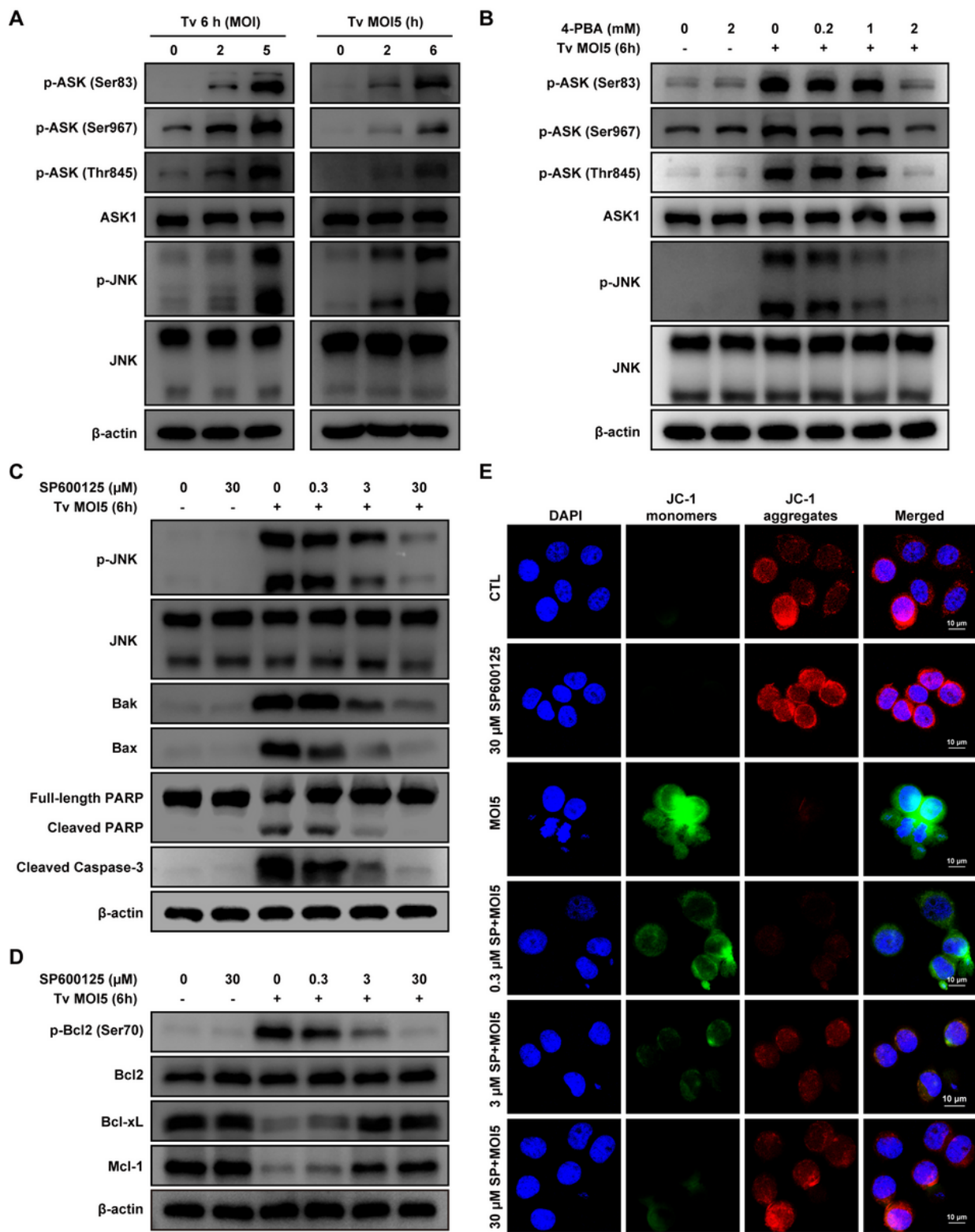


Figure 7

T. vaginalis-induced ES stress-dependent mitochondrial apoptosis via ASK1/JNK pathways in SiHa cells.

(A) SiHa cells were infected with T. vaginalis at the indicated MOI for 6 h or at MOI 5 for the indicated time. Cells were lysed, and the ASK/JNK phosphorylation levels were assessed by western blot analysis.

(B) SiHa cells were pretreated with various concentrations of 4-PBA for 2 h, and subsequently infected with T. vaginalis at MOI 5 for 6 h. ASK/JNK phosphorylation levels were assessed by western blot

analysis. (C-E) SiHa cells were pretreated with various concentrations of a JNK inhibitor (SP600125) for 2 h, and subsequently infected with *T. vaginalis* at MOI 5 for 6 h. The protein levels of JNK, Bak, Bax, cleaved PARP and caspase 3 (C), p-Bcl-2 (Ser70), Bcl-2, Bcl-xL, and Mcl-1 (D) were assessed using western blotting analysis. Anti- β -actin was used as an internal control. JC-1 staining was observed by confocal imaging (E). All the results presented are representative of three independent experiments with similar results.

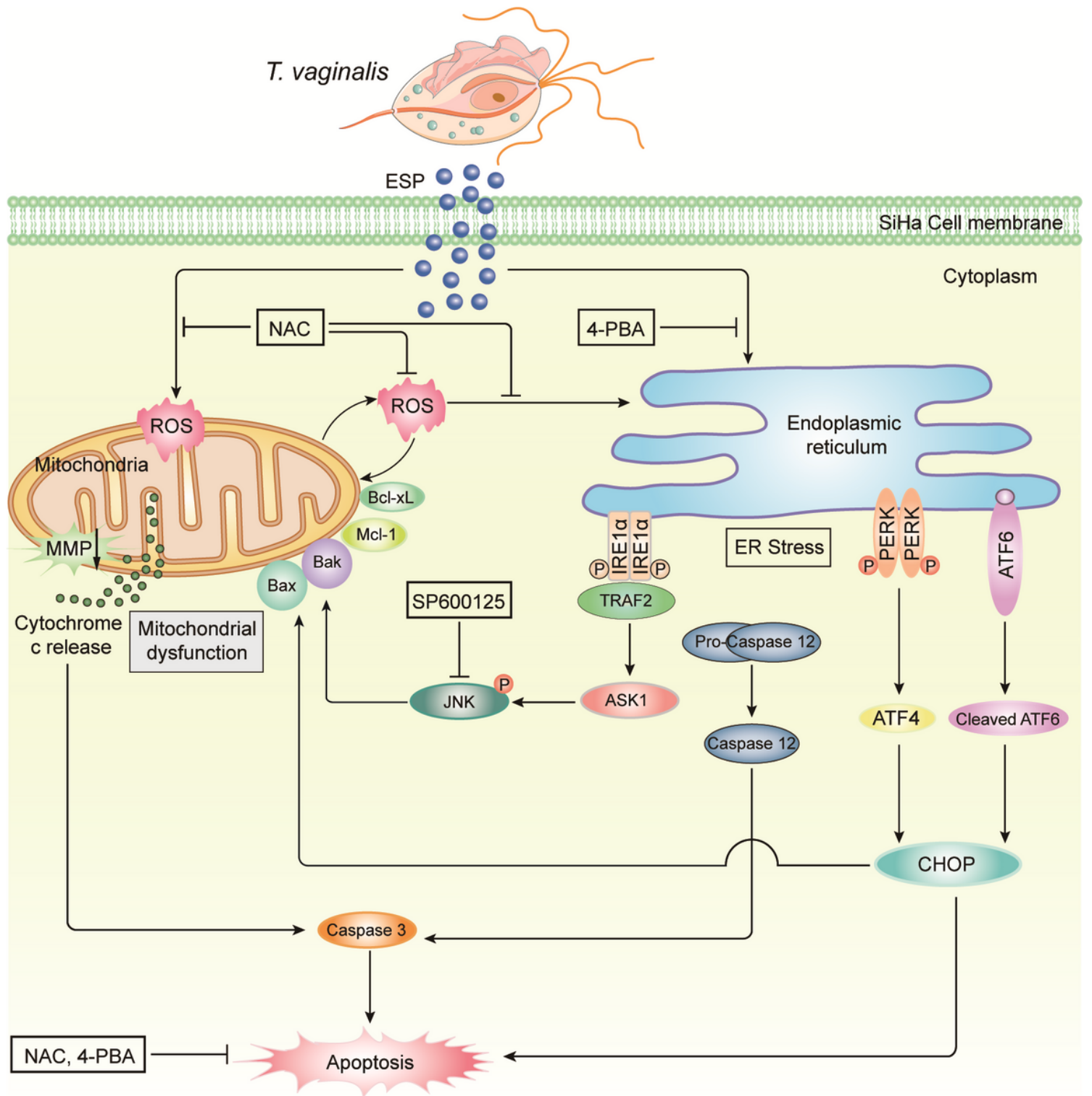


Figure 8

Schematic model of apoptosis by *T. vaginalis* infection in SiHa cells. *T. vaginalis* induces mitochondrial ROS generation and ER stress response. *T. vaginalis* also induces ROS-dependent ER stress response and ER stress-mediated mitochondrial dysfunction, finally leading to apoptosis of the SiHa cells. Thus, *T. vaginalis* infection induces apoptosis via ROS-ER stress-mitochondrial apoptosis pathways by interaction with mitochondria and ER in human cervical epithelium.

Supplementary Files

This is a list of supplementary files associated with this preprint. Click to download.

- [ParaVectorsTvAdditionalfile1sub20210315.docx](#)
- [ParaVectorsTvAdditionalfile2sub20210315.docx](#)
- [ParaVectorsTvGraphicalabstractsub20210315.png](#)